Synthesis and Swelling Properties of Guar Gum-*g*-poly(sodium acrylate)/ Na-montmorillonite Superabsorbent Nanocomposite

WENBO WANG[1,2] AND AIQIN WANG[1,*]

[1]*Center of Eco-material and Green Chemistry, Lanzhou Institute of Chemical Physics Chinese Academy of Sciences, Lanzhou 730000, P.R. China*

[2]*Graduate University of the Chinese Academy of Sciences, Beijing 100049, P.R. China*

ABSTRACT: Novel guar gum-*g*-poly(sodium acrylate)/Na-montmorillonite (GG-*g*-PNaA/MMT) superabsorbent nanocomposites were synthesized by grafted copolymerization among natural guar gum (GG), partially neutralized acrylic acid (NaA) and Na-montmorillonite (MMT) in the aqueous solution using ammonium persulfate as initiator and *N,N′*-methylenebisacrylamide (MBA) as crosslinker. Fourier transform infrared spectroscopy confirmed that NaA had been grafted onto GG and the –OH groups of MMT participated in the reaction. X-ray diffraction and scanning electron microscopy analyses revealed that MMT was exfoliated and equably dispersed in GG-*g*-PNaA matrix. The effects of MMT and MBA on water absorbency were investigated. The results show that introducing MMT into the GG-*g*-PNaA network improved the swelling capability and the swelling rate of the superabsorbent nanocomposite. The nanocomposites keep water absorbency high, within a wide pH range from 4 to 11 and exhibit better reswelling capability.

KEY WORDS: guar gum, montmorillonite, superabsorbent nanocomposite, swelling.

INTRODUCTION

SUPERABSORBENTS CAN ABSORB and retain huge volumes of aqueous liquids compared with traditional absorbing materials, which have been potentially applied in various areas such as agriculture [1,2], hygienic products [3], wastewater treatment [4,5], etc. However, there are limitations to such applications because most of superabsorbent used in practice are expensive synthetic polymer, their production consumes a lot of

*Author to whom correspondence should be addressed. E-mail: aqwang@lzb.ac.cn

0021-9983/09/23 2805–15 $10.00/0 DOI: 10.1177/0021998309345319

petroleum resources and their usage also cause a nonnegligible environmental problem [6]. Thus the utilization of raw materials available in nature for deriving superabsorbent materials has became a subject of great interest, and recently the organic–inorganic nanocomposites based on natural polymer and the inorganic layered silicates have been especially, concerned in both academia and industry. The substitute of the low cost, annually renewable, and biodegradable natural polymer such as polysaccharides for petroleum-based polymers has offered commercial and environmental advantages [7], and the incorporation of inorganic layered silicates into pure polymeric networks with uniform dispersion can not only reduce the production cost, but also can improve the water-absorbing properties and the gel strength of the resultant absorbing materials [8]. Therefore, the composite of natural polysaccharides with inorganic layered silicates are the promising fields. Presently, natural macromolecules such as starch [9,10], cellulose [11], chitosan [12,13], gelatin [14], alginate [15], etc. and their derivatives have been used as polymer matrix for preparing superabsorbents, and the resulting materials also exhibited ameliorative properties.

Guar gum (GG), as a representative natural vegetable gum, is a branched biopolymer with β-D-mannopyranosyl units linked (1-4) with single-membered α-D-galactopyranosyl units occurring as side branches (Scheme 1). GG and their derivatives have been used in many areas (e.g., thickeners, ion exchange resin, suspending agent, etc.). However, only few researches focusing on the introduction of GG into the superabsorbents have taken place. Na-montmorillonite (MMT) belongs to the family of 2 : 1 layered silicates with active –OH groups and exchangeable cations. It can dilate in polar-media and disperse in composites at nanoscale and thus enhancing various abilities of materials [16]. The chemical composite of GG and MMT was expected to improve the network structure and the comprehensive performance of the resulting superabsorbent materials.

On the basis of our previous work about organic–inorganic superabsorbent composites [17,18], in this work, we report the synthesis of superabsorbent nanocomposites by the graft copolymerization of GG and NaA in the presence of MMT micropowder. The nanocomposites were characterized by Fourier transform infrared (FTIR) spectra, X-ray diffraction (XRD), and scanning electron microscopy (SEM). The effects of MMT and *N,N′*-methylenebisacrylamide (MBA) content on water absorbency of the nanocomposite hydrogels were investigated. Also, the swelling behaviors of the developed nanocomposites in saline solution, various pH solutions, and reswelling capability were studied systematically.

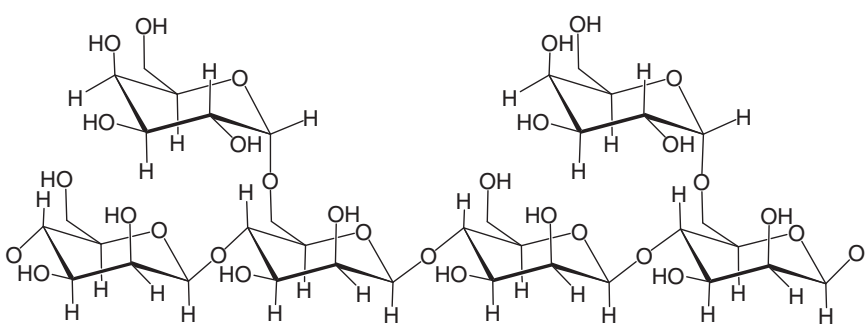

Scheme 1. *Chemical structures of natural GG.*

EXPERIMENTAL

Materials

GG (food grade, number average molecular weight 220,000) was from Wuhan Tianyuan Biology Co., China. Acrylic acid (AA, chemically pure, Shanghai Shanpu Chemical Factory, Shanghai, China) was distilled under reduced pressure before use. Ammonium persulfate (APS, analytical grade, Xi'an Chemical Reagent Factory, China) was used as received. MBA (chemically pure, Shanghai Chemical Reagent Corp., China) was used as purchased. Na-MMT was from the Longfeng Montmorillonite Corporation (Shandong, China) and was passed through 320-mesh screen before use. All other reagents were of analytical grade and all solutions were prepared with distilled water.

Preparation of GG-*g*-PNaA/MMT and GG-*g*-PNaA Superabsorbents

GG (1.20 g) was dispersed in 34 mL of NaOH solution (pH = 12.5, 0.067 mol/L; calculated as a part of neutralization degree) in a 250 mL four-necked flask equipped with a mechanical stirrer, a reflux condenser, a thermometer, and a nitrogen line. The resulting dispersive mixture was heated to 60°C in an oil bath for 1 h to form colloidal slurry. An aqueous solution (4 mL) containing initiator APS (0.1008 g) was then added to the slurry and was stirred at 60°C for 10 min to generate radicals. After the reactants were cooled to 40°C, a mixed solution composing 7.2 g AA (neutralized by 8.5 mL, 8 mol L^{-1} NaOH solution), 0.0216 g of crosslinker MBA, and calculated amounts of MMT powder was added, and then the oil bath was slowly heated to 70°C and kept for 3 h. A nitrogen atmosphere was maintained throughout the reaction period. The obtained products were dried in an oven at 70°C to a constant weight; the dried samples were ground and kept at particle size from 40 to 80 mesh. GG-*g*-PNaA superabsorbent hydrogel was prepared according to a similar procedure but without MMT.

Measurements of Equilibrium Water Absorbency and Swelling Kinetics

A 0.05 g of sample was immersed in excessive aqueous liquids for 4 h to reach swelling equilibrium. The swollen gels were filtered out using a mesh screen, and then drained on the sieve for 10 min. After weighing the swollen samples, the equilibrium water absorbency of the superabsorbent was calculated using the following equation:

$$Q_{eq} = (w_s - w_d)/w_d \quad (1)$$

where Q_{eq} is the equilibrium water absorbency (g/g), which is the averages of three measurements; w_d and w_s are the weights of the dry sample and the swollen sample, respectively. All samples were weighed three times repeatedly and the average values are reported in this article.

Swelling kinetics of the superabsorbents in saline solutions with various concentrations were measured as follows: an accurate amount of samples (0.05 g) were placed in 500 mL beakers, into which 100 mL of saline solutions was then poured. The swollen gels were filtered out using a sieve at set intervals, and the water absorbency of superabsorbents at a certain moment was measured by weighing the swollen and the dry samples and was calculated according to Equation (1).

Reswelling Capability

The sample (0.05 g) was soaked in 100 mL of distilled water to achieve the swelling equilibrium, and then the swollen sample was placed in an oven to dehydrate at 100°C. After being dried thoroughly, an equal volume of water was added to the recovered superabsorbent to reach swelling equilibrium. The swollen samples were dehydrated by above procedure again. Similar procedure was repeated for several times to evaluate the reswelling capabilities of superabsorbents.

Characterizations

The FTIR spectra were recorded on a Nicolet NEXUS FTIR spectrometer in 4000–400 cm^{-1} region using KBr pellets. XRD analyses were performed using an X-ray power diffractometer with Cu anode (PAN analytical Co. X'pert PRO), running at 40 kV and 30 mA, scanning from 3° to 15° at 3° min^{-1}. The morphologies of the samples were examined using a JSM-6701F field emission scanning electron microscope (JEOL) after coating the sample with gold film.

RESULTS AND DISCUSSION

The superabsorbent nanocomposite network can be formed through the grafting polymerization and chemically crosslinking reaction of GG, NaA, and MMT, the proposed mechanism is depicted in Scheme 2. At the stage of initiation, the initiator APS was decomposed under heating to generate sulfate anion-radicals, and then these radicals strip down the hydrogen of –OH groups on GG or MMT to form alkoxy radicals. These radicals can act as the active centers during the reaction and can initiate NaA to process chain propagation. In the course of chain propagation, the crosslinker MBA containing vinyl groups and MMT containing active –OH (forming ester with carboxyl) also participates in the grafting copolymerization, which makes the copolymer form a crosslinked network structure.

FTIR Spectra

The FTIR spectra of (a) MMT, (b) GG, (c) GG-*g*-PNaA, (d) GG-*g*-PNaA/MMT, (e) the physical mixture of GG and PNaA (the weight ratio of PNaA to GG is 6), and (f) the physical mixture of GG-*g*-PNaA and MMT (the weight ratio of GG-*g*-PNaA to GG is 16) were shown in Figure 1. As can be seen from Figure 1(b), the characteristic absorption peaks of GG at 1013, 1077, and 1153 cm^{-1} are ascribed to the stretching vibrations of the C–OH and the band at 1642 cm^{-1} is ascribed to the bending vibration of –OH groups. After graft-copolymerization with NaA, these absorption peaks of GG almost disappeared (Figure 1(c)); however, these characteristic peaks can be observed clearly in the spectrum of the physical mixture of GG and PNaA, indicating that GG has reacted with NaA by its active –OH groups. Moreover, GG-*g*-PNaA has new peaks appearing at 1559, 1452, and 1407 cm^{-1}, respectively, which is attributed to be asymmetric stretching and symmetric stretching of $-COO^-$ groups. This information indicates NaA had been grated onto GG backbone. The characteristic peaks of MMT at 3697 and 3621 cm^{-1} as well as at 1636 cm^{-1} (Figure 1(a)) are ascribed to the stretching vibration and the bending vibration

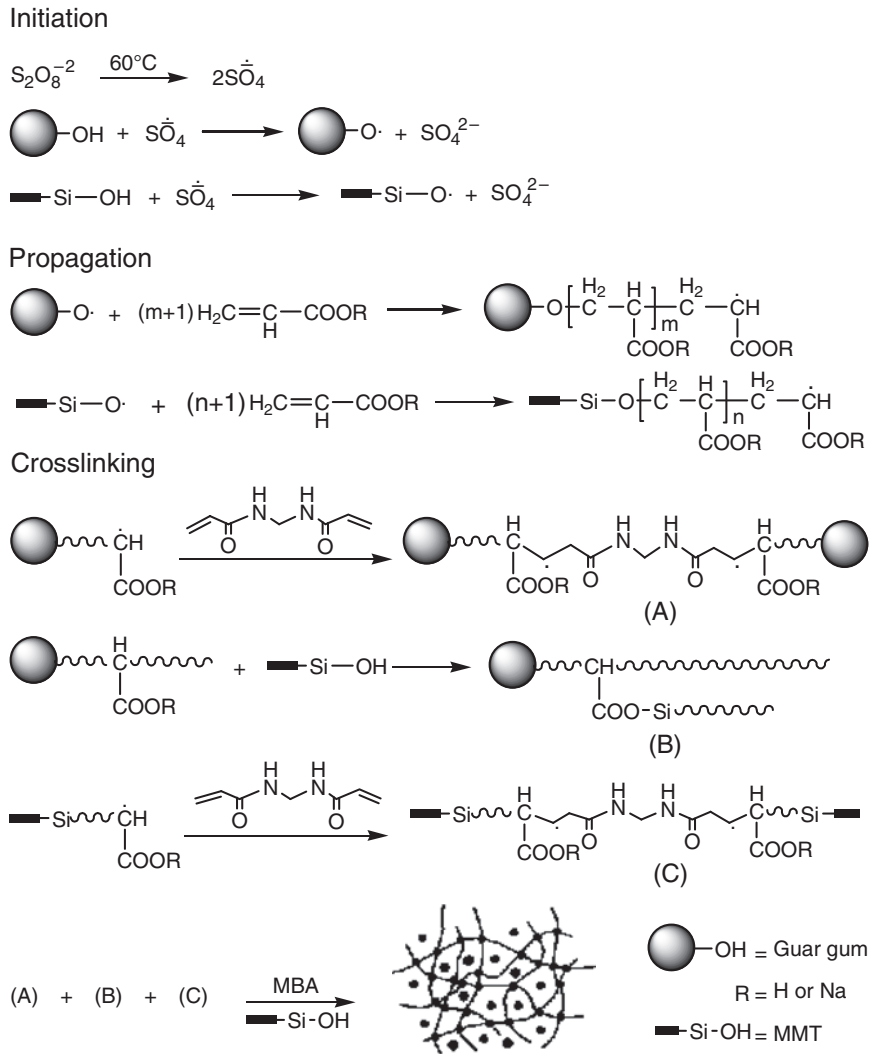

Scheme 2. *Proposed mechanisms for the formation of superabsorbent composite network.*

of –OH on the surface of layers of MMT, respectively, which disappeared in the spectrum of the GG-*g*-PNaA/MMT superabsorbent nanocomposite (Figure 1(d)). The absorption band of MMT at 1033 cm^{-1} attributed to Si–O stretching appeared in the spectrum of GG-*g*-PNaA/MMT and are obviously weakened after polymerization reaction. However, the stretching vibration bands of –OH groups on MMT at 3621 and 3697 cm^{-1} and the Si–O stretching at 1033 cm^{-1} are present in the spectrum of the physical mixture of GG-*g*-PNaA and MMT (Figure 1(f)) with a considerable intensity, and the peak positions are close with that of MMT. By comparison with Figure 1(d) and Figure 1(f), it can be concluded that MMT is not mixed physically with GG-*g*-PNaA during the polymerization reaction and the chemical reaction occurred among GG, NaA, and MMT. Furthermore, the C=O bands of GG-*g*-PNaA at 1627 cm^{-1} shifted to 1634 cm^{-1} after forming GG-*g*-PNaA/MMT, which implied the occurrence of esterification between MMT and

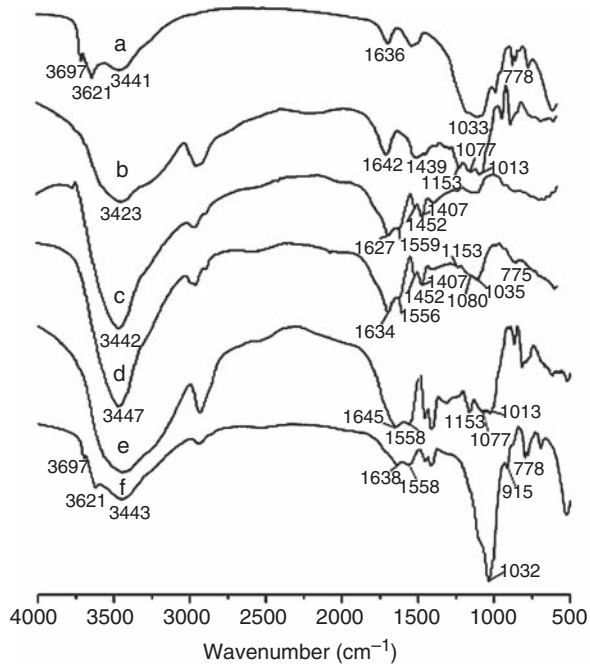

Figure 1. *FTIR spectra of (a) MMT, (b) GG, (c) GG-g-PNaA, (d) GG-g-PNaA/MMT (5 wt%), (e) the physical mixture of GG and PNaA, and (f) the physical mixture of GG-g-PNaA and MMT.*

PNaA (Scheme 2). As a whole, the above analysis results indicate that the MMT also participated in the grafting copolymerization reaction through its active ≡Si–OH groups [19].

XRD Analyses

XRD patterns of MMT and GG-*g*-PNaA/MMT (5 and 20 wt%) were collected from 3° to 15° (2θ) and shown in Figure 2. It can be observed that the natural MMT shows a strong characteristic peak at $2\theta = 7.01°$ with a basal spacing of 1.2611 nm. However, no obvious peak can be observed in the XRD curves of the nanocomposites even if the content of MMT reaches 20 wt%. As well-known, the changes in the data of crystallochemical parameters derived from 001 peak analysis is the criterion, by which the intercalated or exfoliated composite can be decided [20,21]. The absence of characteristic peaks of MMT in the nanocomposites indicated that the platelets of MMT have almost been exfoliated and are thoroughly dispersed in the polymer matrix at nanoscale after polymerization [22,23], forming a composite structure. The similar result can also be observed in the nanocomposite superabsorbent starch grafted P(AA-*co*-AM)/MMT [24].

Morphological SEM

SEM micrographs of superabsorbent containing various amounts of MMT were observed and are shown in Figure 3. As can be seen, the superabsorbent hydrogel of GG-*g*-PNaA exhibits smooth and dense surface (Figure 3(a)); while the superabsorbent nanocomposites incorporated various amounts of MMT and all show a relatively coarse

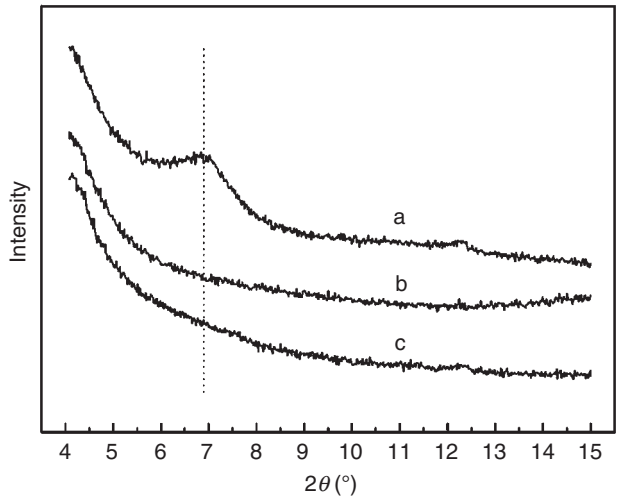

Figure 2. *XRD patterns of (a) MMT, (b) GG-g-PNaA/MMT (5 wt%), and (c) GG-g-PNaA/MMT (20 wt%).*

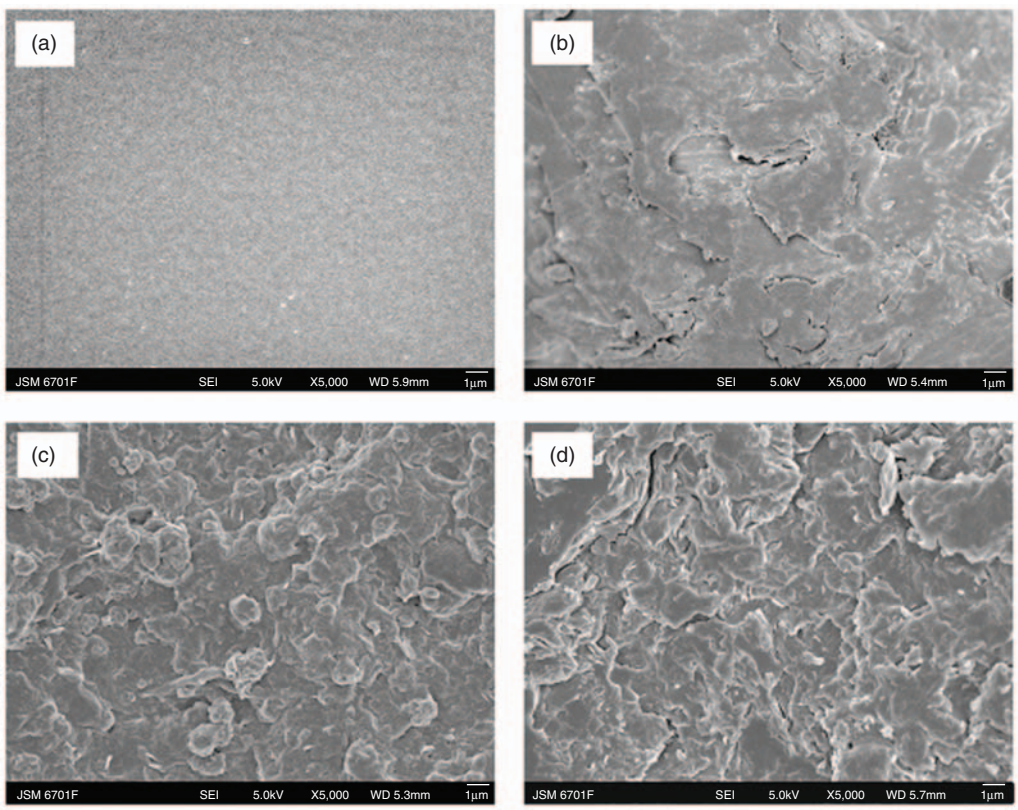

Figure 3. *SEM micrographs of (a) GG-g-PNaA, (b) GG-g-PNaA/MMT (5 wt%), (c) GG-g-PNaA/MMT (10 wt%), and (d) GG-g-PNaA/MMT (20 wt%).*

and loose pleat surface (Figure 3(b)–(d)). It can also be observed that the surface roughness of superabsorbent nanocomposites increases with the increase in the content of MMT. The nanocomposite containing 5 wt% of MMT only had shown a slightly coarse and undulant surface, no obvious pleats can be observed (Figure 3(b)). However, with the further increase in the content of MMT, the surface roughness was obviously improved and the pleat structure was also observed, and some pores and gaps were also observed in the surface of the nanocomposite containing 20 wt% of MMT. The degree of dispersion of clay micropowder in the polymer matrix is more important for an organic–inorganic composite [25]. Thus, this observation also gives a direct revelation that the MMT are almost embedded within GG-*g*-PNaA and uniformly dispersed in the polymer matrix (Figure 3(b)–(d)). The fine dispersion of MMT particles in the polymer network prevents flocculation of clay particles and facilitates the resulting superabsorbent to form a homogeneous composition, which is accordant with the XRD results that MMT disperses in matrix with exfoliated platelets (Figure 2).

Effects of MMT Content on Water Absorbency

MMT content has greater influence on the water absorbency of the resultant superabsorbent nanocomposites because MMT can participate in the construction of 3D network. As shown in Figure 4, the water absorbency of superabsorbent nanocomposite remarkably increases by 42%, in contrast to the sample without MMT, when 5 wt% of MMT was introduced. This result can be attributed to the following reasons: MMT contains large amounts of active –OH groups on its layer surface. During polymerization, MMT was exfoliated and its layers were equably dispersed in the polymeric matrix (Figures 2 and 3). According to previous report [22] and the FTIR analyses (Figure 1), the MMT layers can participate in grafting copolymerization reaction through the active –OH groups on its surface (Scheme 2). On the one hand, the composite of MMT with polymeric matrix improved the surface structure and increased the surface area of superabsorbent (Figure 3); on the other hand, the introduction of rigid MMT layer also

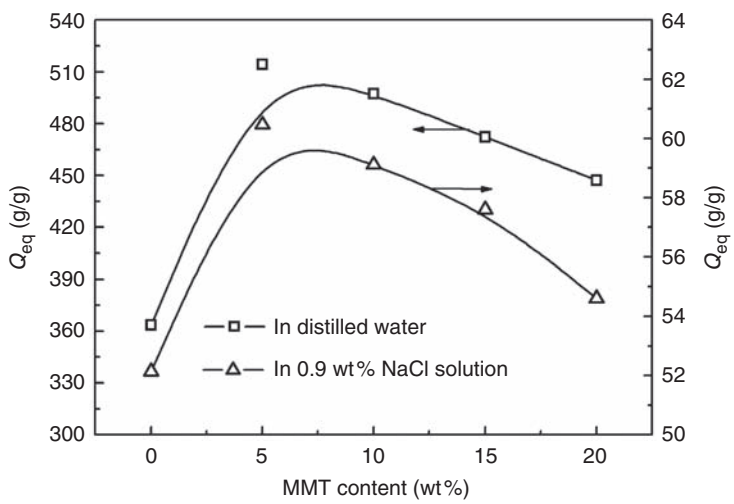

Figure 4. *Effects of MMT content on the water absorbency.*

prevents the intertwist of graft polymer chains and weaken the hydrogen-bonding interaction among the –COOH groups on polymeric chains, and then decrease the degree of physical crosslinking. As a result, the water absorbency was enhanced due to the incorporation of MMT. However, the water absorbency gradually decreased with the further increase of MMT content from 5 to 20 wt%. This result may be attributed to the facts that, (1) according to Lin et al. [26], ultrafine clay powder can act as an additional crosslinking point in the polymeric network. Thus, the introduction of MMT into polymeric network may increase the crosslinking density of superabsorbent and minimize the network space for holding water; (2) the water absorbency is also related to affinity of the superabsorbent with water. When introducing excess MMT, the exfoliated layers may physically stack in network space, which decreased the ratio of hydrophilic groups in unit volume and lead to the decrease of hydrophilicity of superabsorbent nanocomposite. As a result, the water absorbency decreased with the further increase of MMT content. The similar tendency can also be observed in starch-graft-AA/Na-MMT [23]. In addition, it is worthy pointing out that the water absorbency of superabsorbent nanocomposite incorporated with 20 wt% of MMT is still 23% higher than sample without MMT; this is favorable to reduce the production cost.

Effects of MBA Concentration on Water Absorbency

As well-known, the concentration of crosslinker usually exhibits more notable effects on the water absorbency than others. It can be seen from Figure 5 that the water absorbency of superabsorbent nanocomposite sharply decreases with the increase in MBA concentration from 2.55 to 8.49 mmol L^{-1}. According to Flory's theory [27], the water absorbency of the superabsorbent is closely related to crosslinked density. In radical polymerization, a high crosslinker concentration will cause the generation of more crosslinking points and the increase of crosslinked density. As a result, the network space left for holding water was minimized and the water absorbency decreased. As described previously [28],

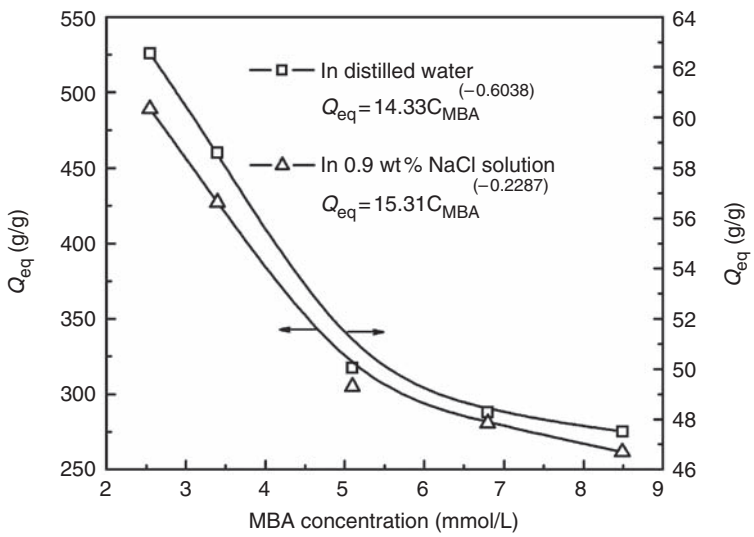

Figure 5. *Effects of MBA concentration on the water absorbency.*

the equilibrium water absorbency of superabsorbent was found to follow a power law relation with MBA concentration (Equation (2)):

$$Q_{eq} = kC_{MBA}^{(-n)} \tag{2}$$

where Q_{eq} is equilibrium water absorbency; C_{MBA} is the concentration of crosslinker MBA; k and n are power law constants for an individual superabsorbent, which can be obtained from the curve fitted with Equation (2). For superabsorbent nanocomposite GG-*g*-PNaA/MMT, the relation between Q_{eq} and C_{MBA} follows the equations $Q_{eq} = 14.33C_{MBA}^{(-0.6038)}$ in distilled water and $Q_{eq} = 15.31C_{MBA}^{(-0.2287)}$ in 0.9 wt% NaCl solution.

Effects of Saline Solutions on Water Absorbency

The effect of saline solution on the swelling behaviors of superabsorbent nanocomposite was measured in NaCl solution and the swelling curves were shown in Figure 6(a). It can be seen that the swelling rate of the superabsorbent nanocomposite in each solution is high within 900 s, and then the swelling rate decreased and the swelling kinetic curves became flatter. In this section, the swelling kinetics of the superabsorbent nanocomposite in saline solution with various concentrations were expressed by the Scott's second-order swelling kinetics model (Equation (3)) [29]:

$$t/Q_t = A + Bt \tag{3}$$

where Q_t is the water absorbency at a given time t; $B = 1/Q_\infty$ is the inverse of equilibrium water absorbency; $A = 1/K_s Q_\infty^2$ is the reciprocal of the initial water-absorbing rate of the superabsorbent nanocomposite, and K_s is swelling rate constant. The final form of equation will be as follows:

$$t/Q_t = 1/K_s Q_\infty^2 + 1/Q_\infty^t \tag{4}$$

On basis of the experimental data, the plots of t/Q_t vs. t give perfect straight lines with good linear correlation coefficient (>0.99; Figure 6(b)), indicating that the swelling of superabsorbent nanocomposite observes the Scott's swelling theoretical model. Also, by fitting experimental data using Equation (4), the swelling kinetic parameters including the swelling rate constant (K_s), the theoretical equilibrium water absorbency (Q_∞) and the initial swelling rate ($K_{is} = K_s Q_\infty^2$) can be calculated by the slope and intercept of lines (Figure 6(b)), and the results are listed in Table 1. It can be noticed that the initial swelling rate constant (K_{is}) of the superabsorbent nanocomposite rapidly decreased from 5.1070 to 1.0486 with the enhancing external saline concentration. This tendency can be ascribed to the fact that the increase of external ionic strength directly leads to the decrease in the osmotic pressure difference between gel network and external solution. At the initial stage of swelling, the diffusion of water into polymeric network is the rate-limiting process, and the osmotic pressure difference act as a driving force for this process. So, increasing the external ionic strength certainly induces the decrease of diffusion rate. However, the swelling rate constant K_s takes on reversed tendency comparing with the initial swelling rate constant K_{is}; K_s increased with increase in the external ionic strength. It is well known that increasing the external saline concentration induce the diminish of electroelastic forces among polymeric chains due to the screening effects of cations penetrating into gel network, which can affect greatly the swelling capability of superabsorbent. The shrinkage of water absorbency at high saline

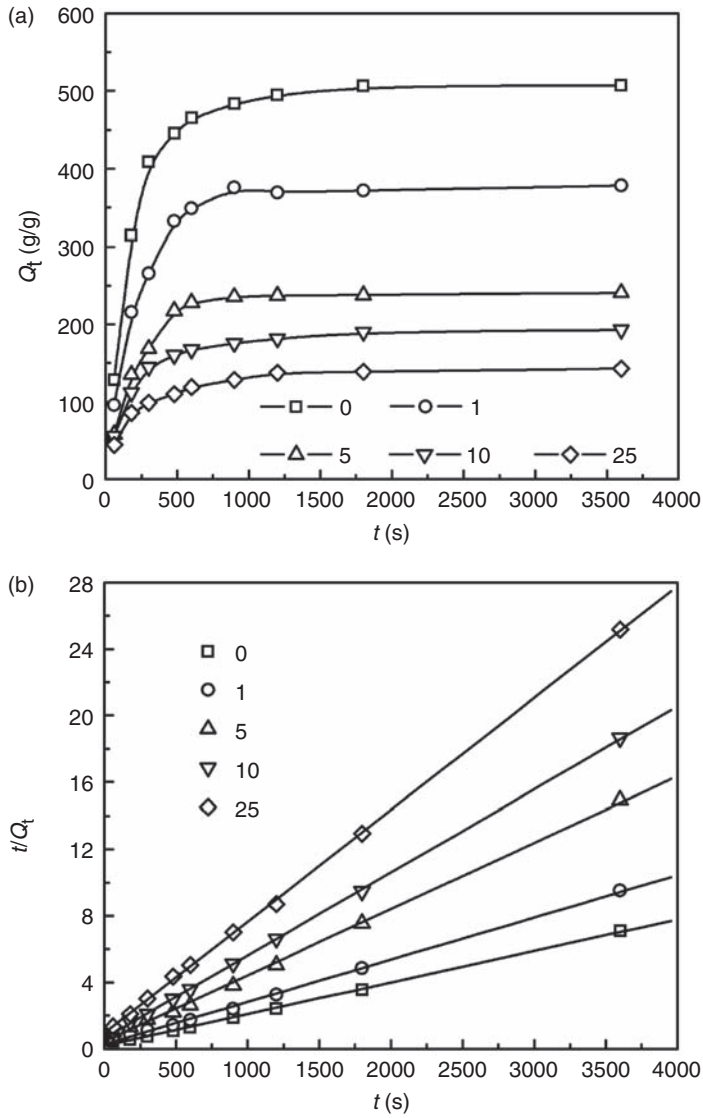

Figure 6. *Swelling kinetic curves (a) and t/Q_t vs. t graphs (b) of GG-g-PNaA/MMT (5 wt%) in saline solution with various concentrations.*

Table 1. Swelling kinetic parameters of GG-g-PNaA/MMT (5 wt%) in saline solutions with various concentrations.

C_{saline} (mmol/L)	Q_{eq} (g/g)	Q_∞ (g/g^1)	K_{is} (g/g/s)	K_s($\times 10^{-5}$, g/g/s)
0	508	526	5.1070	1.9868
1	378	393	3.4395	2.4072
5	241	251	2.2105	3.8059
10	193	201	1.5586	4.1842
25	143	149	1.0486	5.1276

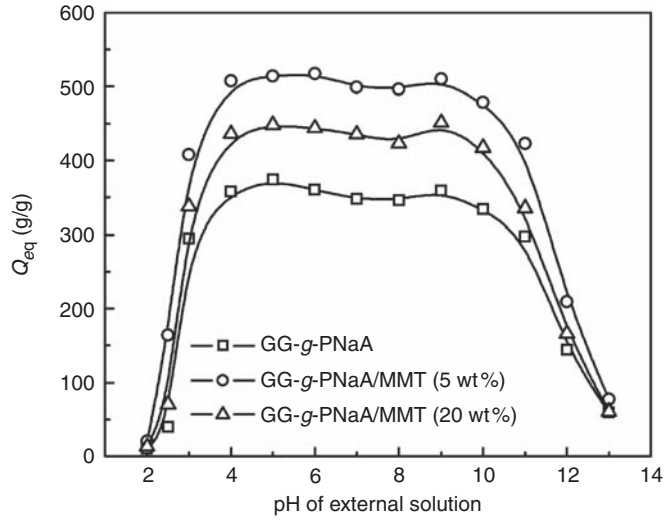

Figure 7. *Effect of external pHs on the water absorbency of superabsorbent nanocomposites.*

concentration means that the polymer chains only need to move lesser distance for reaching the swelling equilibrium, so the time of reaching equilibrium was greatly curtailed.

In addition, it can also been seen that the water absorbency abruptly decreased with the increase in saline concentration (Table 1). As described previously [28], the relationship between equilibrium water absorbency (Q_{eq}) and the concentration of saline solution (C_{saline}) follows a law equation $Q_{eq} = kC_{saline}^{(-n)}$. For the superabsorbent nanocomposite GG-*g*-PNaA/MMT (5 wt%), the law relation between Q_{eq} and C_{saline} can be obtained by fitting the experimental data and was described as the equation $Q_{eq} = 379.52C_{saline}^{(-0.2944)}$ ($R^2 = 0.9987$).

Effect of External pHs on Water Absorbency

In the practical application, the sensitivity of superabsorbent to the external pHs is also a nonnegligible influence factor. In this section, the swelling properties of GG-*g*-PNaA/MMT at solutions with various pHs were evaluated and the results are shown in Figure 7. It can be seen that the water absorbency of GG-*g*-PNaA/MMT almost keeps constant at a wide pHs range from 4 to 11, but sharply decreases when the external pHs exceeds this region. As anionic-type superabsorbent, GG-*g*-PNaA/MMT contains numerous dissociable hydrophilic –COOH and $–COO^-$ groups that can transform each other when the external pH values were changed. At acidic condition (pH < 4), the ionized degree of –COOH(Na) groups may increase with the enhancing external pH values, which induce the immediate conversion of –COOH groups to $–COO^-$ groups. As a result, the osmotic swelling pressure and the electrostatic repulsion among negative $–COO^-$ groups also increased [30], and so the gel networks can easily expand and hold more water. At basic condition (pH > 11), the increased ionic strength of external solution causes the rapid decreases of ion osmotic pressure and the abrupt increase of screening effects of cations, which cause the reduction of water-absorbing capability of superabsorbent nanocomposites. It is worth to point that the superabsorbent nanocomposites can reach the absorbing capability that is almost equal to their equilibrium water absorbency in a wide pH range

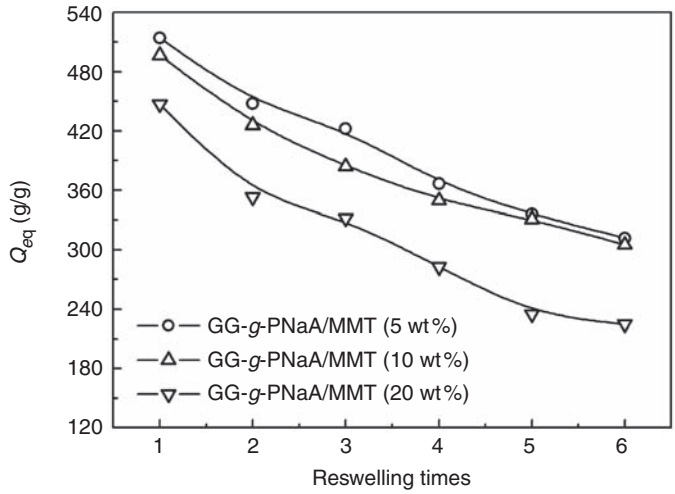

Figure 8. *Water absorbency of the superabsorbent nanocomposite as a function of reswelling times.*

from 4 to 11, this behavior is resulting from the buffer action of –COOH and $–COO^-$ groups [31], and is advantageous for their application in various type of soil for agricultural and ecological use.

Reswelling Capability

After a thorough dewatering of the swollen superabsorbent, the resulting dry nanocomposites still show a better water-absorbing capability than the sample without MMT. Figure 8 shows the equilibrium water absorbencies for GG-*g*-PNaA/MMT superabsorbent nanocomposites in distilled water as a function of reswelling times. As can be seen, the water absorbencies for superabsorbent nanocomposites decrease with increasing reswelling times, and the water absorbency of the superabsorbent nanocomposites is always in the order: GG-*g*-PNaA/MMT (5 wt%) > GG-*g*-PNaA/MMT (10 wt%) > GG-*g*-PNaA/MMT (20 wt%). It can also be observed that the nanocomposites still retain approximately 60.47% (5 wt% MMT), 61.46% (10 wt% MMT), and 50.31% (20 wt% MMT), of their initial water absorbency after reswelling for six times (the heating oven test repeated five times at 100°C), indicating that the superabsorbent nanocomposites still retain a high degree of water-absorbing ability. These results also give direct implication that the superabsorbent composites are reusable and recyclable water-absorbing materials, and can be used as potential ecological materials.

CONCLUSIONS

As a part of the efforts to reduce the excessive consumption of petroleum-based polymer and the environmental impact resulting from the industrial products, a series of GG-*g*-PNaA/MMT superabsorbent nanocomposites were synthesized based on natural GG and MMT. FTIR, XRD, and SEM analyses indicate that MMT was exfoliated during polymerization and equally dispersed in GG-*g*-PNaA matrix at a nanosize, and participates in polymerization reaction through active –OH groups. The MMT content

and MBA concentration exhibit greater influence on the water absorbency of superabsorbent nanocomposites, the sample containing 5 wt% MMT gives the best water absorbency of 514 g/g in distilled water and 61 g/g in 0.9 wt% NaCl solution. The swelling kinetics of the superabsorbent nanocomposite in saline solutions obey Scott's kinetic model, the initial swelling rate constant (K_{is}) decrease with the increase of saline concentration, but the swelling rate constant (K_s) for a long period takes on a reversed tendency. The nanocomposites can keep water absorbency high at a wide pH range from 4 to 11, which are advantageous for their potential application in agriculture. Moreover, the superabsorbent nanocomposites show better reswelling capabilities, the sample containing 10 wt% can retain 61.46% of its initial water absorbency after reswelling for six times. The superabsorbent nanocomposites based on renewable and biodegradable natural polymer and inorganic clay resources exhibited improved water-absorbing capability, water-absorbing rate, pH-resistant and reswelling properties, and can be used as potential water-manageable materials.

ACKNOWLEDGMENTS

This work was financially supported by the Western Action Project of CAS (No. KGCX2-YW-501) and '863' Project of the Ministry of Science and Technology, P. R. China (No. 2006AA03Z0454 and 2006AA100215).

REFERENCES

1. Karada, E., Saraydin, D., Caldiran, Y. and Güven, O. (2000). Swelling Studies of Copolymeric Acrylamide/Crotonic Acid Hydrogels as Carriers for Agricultural Uses, *Polym. Adv. Technol.*, **11**: 59–68.
2. Chu, M., Zhu, S.Q., Li, H.M., Huang, Z.B. and Li, S.Q. (2006). Synthesis of Poly(acrylic acid)/Sodium Humate Superabsorbent Composite for Agricultural Use, *J. Appl. Polym. Sci.*, **102**: 5137–5143.
3. Kamat, M. and Malkani, R. (2003). Disposable Diapers: A Hygienic Alternative, *Indian J. Pediatr.*, **70**: 879–881.
4. Wang, L., Zhang, J.P. and Wang, A.Q. (2008). Removal of Methylene Blue from Aqueous Solution Using Chitosan-g-poly(acrylic acid)/Montmorillonite Superadsorbent Nanocomposite, *Colloid Surface A*, **322**: 47–53.
5. Kaşgöz, H., Durmus, A. and Kaşgöz, A. (2008). Enhanced Swelling and Adsorption Properties of AAm-AMPSNa/Clay Hydrogel Nanocomposites for Heavy Metal Ion Removal, *Polym. Adv. Technol.*, **19**: 213–220.
6. Kiatkamjornwong, S., Mongkolsawat, K. and Sonsuk, M. (2002). Synthesis and Property Characterization of Cassava Starch Grafted Poly[acrylamide-co-(maleic acid)] Superabsorbent Via γ-irradiation, *Polymer*, **43**: 3915–3924.
7. Pourjavadi, A., Sadeghi, M. and Hosseinzadeh, H. (2004). Modified Carrageenan. 5. Preparation, Swelling Behavior, Salt- and pH-Sensitivity of Partially Hydrolyzed Crosslinked Carrageenan-graft-polymethacrylamide Superabsorbent Hydrogel, *Polym. Adv. Technol.*, **15**: 645–653.
8. Wu, J.H., Wei, Y.L., Lin, J.M. and Lin, S.B. (2003). Study on Starch-graft-acrylamide/Mineral Powder Superabsorbent Composite, *Polymer*, **44**: 6513–6520.
9. Lanthong, P., Nuisin, R. and Kiatkamjornwong, S. (2006). Graft Copolymerization, Characterization, and Degradation of Cassava Starch-g-acrylamide/Itaconic Acid Superabsorbents, *Carbohydr. Polym.*, **66**: 229–245.
10. Wu, J.H., Lin, J.M., Zhou, M. and Wei, C.R. (2000). Synthesis and Properties of Starch-graft-polyacrylamide/Clay Superabsorbent Composite, *Macromol. Rapid. Commun.*, **21**: 1032–1034.

11. Suo, A.L., Qian, J.M., Yao, Y. and Zhang, W.G. (2007). Synthesis and Properties of Carboxymethyl Cellulose-graft-poly(acrylic acid-co-acrylamide) as a Novel Cellulose-based Superabsorbent, *J. Appl. Polym. Sci.*, **103**: 1382–1388.
12. Zhang, J.P., Wang, Q. and Wang, A.Q. (2007). Synthesis and Characterization of Chitosan-g-poly(acrylic acid)/Attapulgite Superabsorbent Composites, *Carbohydr. Polym.*, **68**: 367–374.
13. Mahdavinia, G.R., Zohuriaan-Mehr, M.J. and Pourjavadi, A. (2004). Modified Chitosan III, Superabsorbency, Salt- and pH-sensitivity of Smart Ampholytic Hydrogels From Chitosan-g-PAN, *Polym. Adv. Technol.*, **15**: 173–180.
14. Pourjavadi, A., Hosseinzadeh, H. and Sadeghi, M. (2007). Synthesis, Characterization and Swelling Behavior of Gelatin-g-poly(sodium acrylate)/Kaolin Superabsorbent Hydrogel Composites, *J. Compos. Mater.*, **41**: 2057–2069.
15. Pourjavadi, A., Ghasemzadeh, H. and Soleyman, R. (2007). Synthesis, Characterization, and Swelling Behavior of Alginate-g-poly(sodium acrylate)/Kaolin Superabsorbent Hydrogel Composites, *J. Appl. Polym. Sci.*, **105**: 2631–2639.
16. Ray, S.S. and Okamoto, M. (2003). Polymer/Layered Silicate Nanocomposites: A Review From Preparation to Processing, *Prog. Polym. Sci.*, **28**: 1539–1641.
17. Zhang, J.P., Wang, L. and Wang, A.Q. (2007). Preparation and Properties of Chitosan-g-poly-(acrylic acid)/Montmorillonite Superabsorbent Nanocomposite via In Situ Intercalative Polymerization, *Ind. Eng. Chem. Res.*, **46**: 2497–2502.
18. Li, A., Zhang, J.P. and Wang, A.Q. (2007). Utilization of Starch and Clay for the Preparation of Superabsorbent Composite, *Bioresour. Technol.*, **98**: 327–332.
19. Li, A., Wang, A.Q. and Chen, J.M. (2004). Studies on Poly(acrylic acid)/Attapulgite Superabsorbent Composite. I. Synthesis and Characterization, *J. Appl. Polym. Sci.*, **92**: 1596–1603.
20. Burnside, S.D. and Giannelis, E.P. (1995). Synthesis and Properties of New Poly(dimethylsiloxane) Nanocomposites, *Chem. Mater.*, **7**: 1597–1600.
21. Ahmadi, S.J., Huang, Y.D. and Li, W. (2005). Morphology and Characterization of Clay-reinforced EPDM Nanocomposites, *J. Compos. Mater.*, **39**: 745–754.
22. Liu, P.S., Li, L., Zhou, N.L., Zhang, J., Wei, S.H. and Shen, J. (2007). Waste Polystyrene Foam-graft-acrylic acid/Montmorillonite Superabsorbent Nanocomposite, *J. Appl. Polym. Sci.*, **104**: 2341–2349.
23. Al, E., Güçlü, G., Iyim, T.B., Emik, S. and Özgümüş, S. (2008). Synthesis and Properties of Starch-graft-acrylic acid/Na-Montmorillonite Superabsorbent Nanocomposite Hydrogels, *J. Appl. Polym. Sci.*, **109**: 16–22.
24. Luo, W., Zhang, W., Chen, P. and Fang, Y. (2005). Synthesis and Properties of Starch Grafted Poly[acrylamide-co-(acrylic acid)]/Montmorillonite Nanosuperabsorbent via γ-ray Irradiation Technique, *J. Appl. Polym. Sci.*, **96**: 1341–1346.
25. Santiago, F., Mucientes, A.E., Osorio, M. and Rivera, C. (2007). Preparation of Composites and Nanocomposites Based on Bentonite and Poly(sodium acrylate). Effect of Amount of Bentonite on the Swelling Behaviour, *Eur. Polym. J.*, **43**: 1–9.
26. Lin, J.M., Wu, J.H., Yang, Z.F. and Pu, M.L. (2001). Synthesis and Properties of Poly(acrylic acid)/Mica Superabsorbent Nanocomposite, *Macromol. Rapid. Commun.*, **22**: 422–424.
27. Flory, P.J. (1953). *Principles of Polymer Chemistry*, Cornell University Press, Ithaca, New York.
28. Kabiri, K., Omidian, H., Hashemi, S.A. and Zohuriaan-Mehr, M.J. (2003). Synthesis of Fast-swelling Superabsorbent Hydrogels: Effect of Crosslinker Type and Concentration on Porosity and Absorption Rate, *Eur. Polym. J.*, **39**: 1341–1348.
29. Schott, H. (1992). Swelling Kinetics of Polymers, *J. Macromol. Sci. B*, **31**: 1–9.
30. Kiatkamjornwong, S., Chomsaksakul, W. and Sonsuk, M. (2000). Radiation Modification of Water Absorption of Cassava Starch by Acrylic Acid/Acrylamide, *Radiat. Phys. Chem.*, **59**: 413–427.
31. Lee, W.F. and Wu, R.J. (1996). Superabsorbent Polymeric Materials. I. Swelling Behaviors of Crosslinked Poly(sodium acrylate-co-hydroxyethyl methacrylate) in Aqueous Salt Solution, *J. Appl. Polym. Sci.*, **62**: 1099–1114.